

Design of Permanent Magnet Linear Synchronous Motor Stator to Improve Magnetic Flux Density Profile Toward High Thrust Density Performance

Nor Ashikin Mohd Nasir¹, Fairul Azhar Abdul Shukor^{1(✉)},
Raja Nor Firdaus Kashfi Raja Othman¹, Hiroyuki Wakiwaka²,
and Kuniyisa Tashiro²

¹ Faculty of Electrical Engineering,
Universiti Teknikal Malaysia Melaka, Malacca, Malaysia
{m011620008.student,
fairul.azhar,norfirdaus}@utem.edu.my

² Faculty of Engineering, Shinshu University, Nagano, Japan
{wakiwak,tashiro}@shinshu-u.ac.jp

Abstract. The Permanent Magnet Linear Synchronous Motor (PMLSM) is designed in this paper to solve the drawbacks of the previous designed PMLSM. The previous designed PMLSM has magnetic flux density, B saturation at lower rated current, I . Therefore, to overcome the saturation of the magnetic flux density, the stator of the PMLSM is designed. Apart from that, the design of the stator help to increase the ratio of thrust, F to cogging force, F_{cog} . The design of PMLSM is completed in two stages where in the first stage the best model chosen is the model of $t_{y2} = 3$ mm. The thrust of the model has reduced by 14% from the previous designed PMLSM. The model designed and chosen in second stage is compared with the previous designed PMLSM in terms of it performance index. The designed PMLSM has improved in terms of motor constant square density, G compared to the previous designed PMLSM with the increment of 2%.

Keywords: Magnetic flux density profile · PMLSM · Performance index · Slot opening parameter · Stator design

1 Introduction

Linear motor is used to produce direct linear motion can be either AC or DC type. The linear motor can be constructed either in the flat or cylindrical form. The linear motor structure is not much different from rotary motor where it has both rotor and stator, however in linear motor the moving part is called as mover instead of rotor. In the linear motor, instead of producing torque (rotation force) it produced linear force, F as it is moving along its length.

Linear motor has many advantages compare to rotary motor where it has higher dynamic performance, simpler structure, improve reliability by reducing some parts

and higher efficiency due to the prevention of the motion translation from rotary to linear motion [1] in a linear motion system. Linear motor extensive usage in many linear motion applications also contributed by their good performances such as high speed high accuracy [2], longer life and maintenance-free operation [3] compared to rotary motor or conventional linear motor.

Despite all the advantages yields by the linear motor, it cannot avoid from being stained by its drawbacks such as high cost and cogging. The cost of the linear motor can be high due to the length of the motor stroke [1] and the permanent magnet used in its structure. The permanent magnet from rare-earth material can be very expensive compare to the other magnets material in the permanent magnet markets [4]. Apart from that, linear motor especially from permanent magnet type produced cogging force as there are interaction between the stator core and the permanent magnet mover [5]. The cogging can decrease the motor efficiency, decline motor controllability and reduced motor average thrust force [5].

2 Basic Principle of the PMLSM

The PMLSM designed in this project is a cylindrical 6-slot, 8-pole types with three phases supply. This motor consists of six stator slot and the Halbach magnetization array of PM on its mover as shown in Fig. 1. The PMLSM has been designed previously [1], however the PMLSM yields weakness where there is unbalanced size between the stator and the coil. The unbalance size made the magnetic flux density, B saturated at lower than targeted rated current hence limit the thrust, F produced [1]. Therefore, in this paper, the stator of the PMLSM was designed to improve the performance characteristics of the PMLSM.

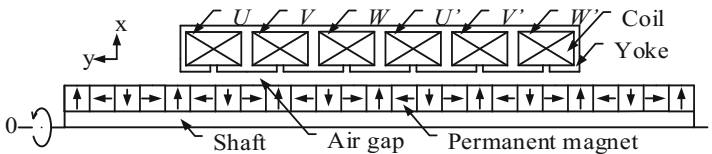


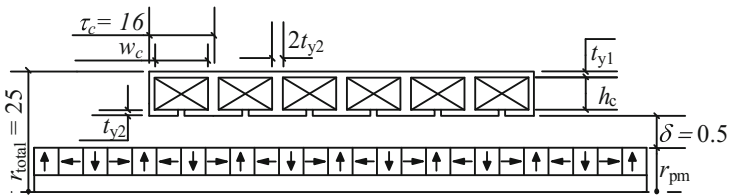
Fig. 1. PMLSM basic structure.

3 Design of the PMLSM Stator

The PMLSM was designed within fixed of outer radius which equal to 25 mm. The structure parameters of the PMLSM is shown in the Table 1. The value of outer radius is fixed because the main purpose of this design is to improve the PMLSM performance by improving its stator part. The general structure of the PMLSM designed in this paper is shown in Fig. 2. During the design, the coil parameters which is coil height, h_c and coil width, w_c were changed accordingly to the changes of the stator yoke thickness, t_{y2} while the other parameters were remain unchanged.

Table 1. PMLSM parameters.

Symbol	Value
PMLSM total radius, r_{total} (mm)	25
Stator height, h_{st} (mm)	11.5
Stator length, l_{st} (mm)	96
Coil height, h_c (mm)	4.5–7.5
Coil width, w_c (mm)	6–12
Permanent magnet radius, r_{pm} (mm)	13
Shaft radius, r_s (mm)	6
Coil pitch, τ_c (mm)	16
Permanent magnet pitch, τ_{pm} (mm)	12
Copper wire diameter, \varnothing_c (mm)	0.337
PM material	NdFeB (N-42)
Stator material	SS400

**Fig. 2.** Design of stator yoke thickness (unit: mm).

The saturation of the magnetic flux density, \mathbf{B} affects the saturation of PMLSM thrust, F . Therefore, to avoid the thrust saturation, the magnetic flux density need to be reduced below its saturation level which is $\mathbf{B} = 1.8$ T based on the stator material B-H curve. The stator part of the PMLSM was design to reduce the magnetic flux density where the design has been completed within two stages as shown in Fig. 3. The design of PMLSM consists of two stages where the first stage was to design the stator yoke thickness while the second stage was to design the stator slot opening. The models designed were then simulated by using finite element method (FEM) software and the performance characteristics were analysed and evaluated to find the best model.

3.1 Design of Yoke Thickness

Figure 4 shows the magnetic flux density profile of the previous model. Due to the saturated of magnetic flux density, \mathbf{B} , the thrust of PMLSM in [1] is saturated at lower aimed rated current. The magnetic flux density, \mathbf{B} was observed on specific area as shown in Fig. 4(a). The saturation of the magnetic flux density, \mathbf{B} is represented by the line $\mathbf{B} = 1.8$ T as shown in the Fig. 4(b) and (c). In the Fig. 4(b) and (c), it shows that the magnetic flux density in the Region 1 is exceeded the saturation line while the

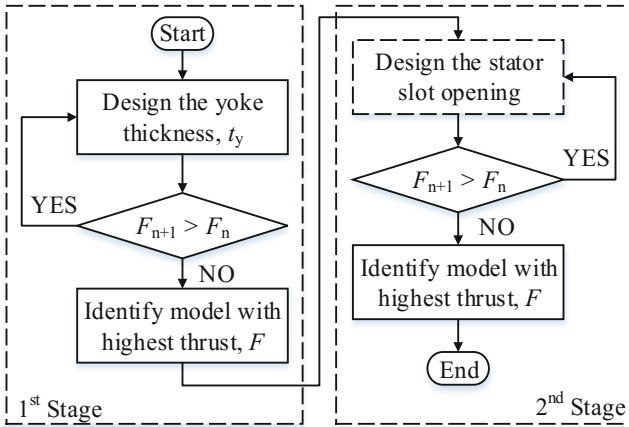


Fig. 3. Flowchart of designing PMLSM stator.

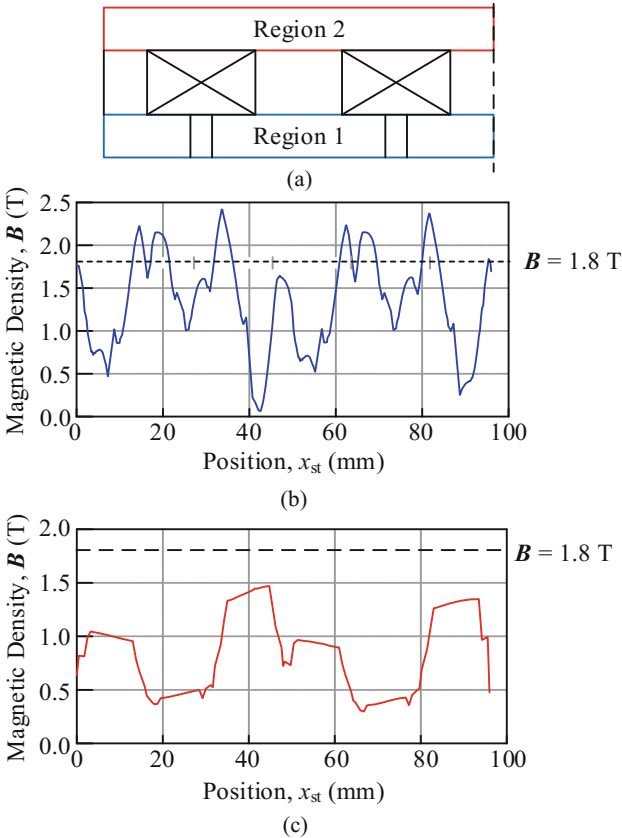


Fig. 4. Magnetic flux density, B of PMLSM. (a) B region of PMLSM stator, (b) B at region 1, (c) B at region 2.

magnetic density, B at Region 2 is lower than the saturation line. Region 1 represents the upper yoke thickness, t_{y1} while Region 2 represents the bottom yoke thickness, t_{y2} . Since the magnetic density, B at Region 2 is already below the saturation line, the design was focused on t_{y2} to decrease the value of the magnetic flux density, B at Region 1.

Figure 5 shows the steps in first stage PMLSM stator design. In the first stage, the designed started by identifying the fixed parameters taken from the previous design [1]. The parameters that were fixed are coil pitch, τ_c , stator height, h_{st} and the upper yoke thickness, t_{y1} . Next was to set the initial value for the variable parameters which is bottom yoke thickness, t_{y2} , coil width, w_c and coil height, h_c to 2 mm, 12 mm and 7.5 mm respectively. The model then was simulated to get the value of thrust, F . The next models were designed by increasing the bottom yoke thickness, t_{y2} by 1 mm for each model until the possible maximum value. The value of coil width, w_c and coil height, h_c were calculated as these parameters were changed accordingly to the changed of bottom yoke thickness, t_{y2} . The models were simulated to capture the thrust, F performance. All the thrust, F obtained from the models designed were evaluated and compared. The final model in first stage was chosen based on the model that produces possible maximum thrust.

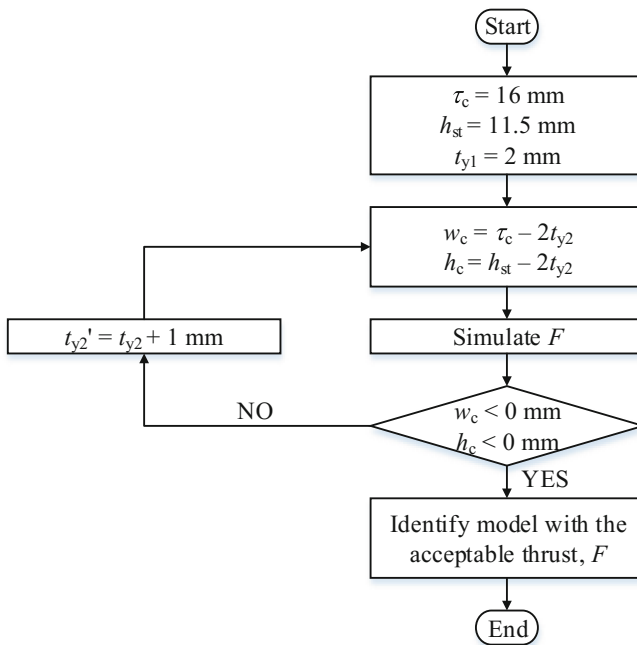


Fig. 5. Flowchart of designing the stator yoke thickness.

3.2 Design of Stator Slot Opening

Model of with yoke thickness, $t_{y2} = 3$ mm has been chosen as the best model from the design in first stage. The model chosen in first stage was used as the initial model in second stage of the PMLSM design. The main objectives of the second stage design is to improve the performance of the models in the first stage design especially in term of cogging force. The best model was determined by choosing the model that can produce the highest thrust, F and the lowest cogging force, F_{cog} . Figure 6 shows the parameters of stator than need to be variable in the second stage.

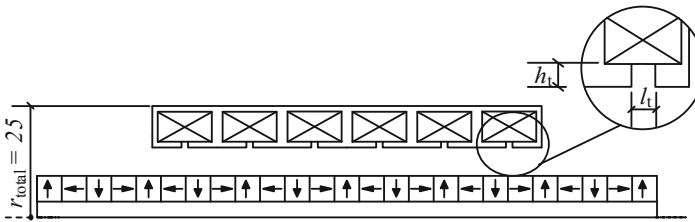


Fig. 6. Design of stator slot opening (unit: mm)

Figure 7 shows the steps taken in second stage of PMLSM design. The second stage design started by identify the structure parameters from the previous stage. In this stage, the parameters identified from the chosen model in previous stage such as yoke thickness, t_y , coil width, w_c , and coil height, h_c were fixed. Next, the initial parameters of stator slot opening which is height of stator slot opening, h_t and length of stator slot

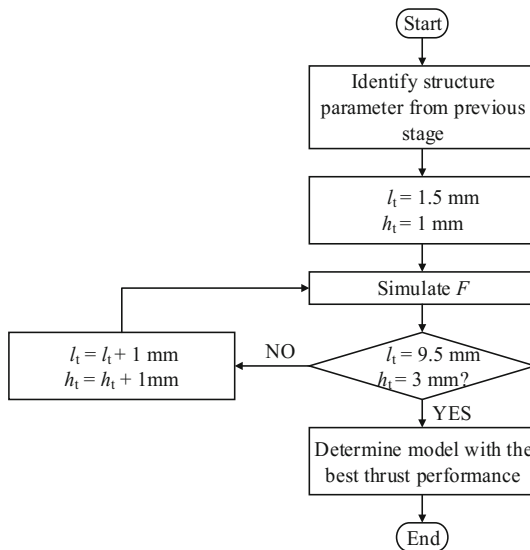


Fig. 7. Flowchart of designing stator slot opening.

opening, l_t were set. The model then simulated to capture the thrust, F . The design was continued by increasing the value of l_t and h_t by 1 mm for each model until the final set value which is $l_t = 9.5$ mm, $h_t = 3$ mm. All the thrust, F obtained from the simulation results were compared to determine the model that satisfy the design's objectives requirement.

4 Analysis of the PMLSM Performance

The design of PMLSM was completed in two stages. The first stage is to design the stator yoke thickness and the second stage is to design the stator slot opening parameters. The performance of the models designed was evaluated based on the magnetic flux density, B , thrust, F characteristics, cogging force, F_{cog} and the thrust ratio of thrust to cogging force. Apart from that, the performance of the PMLSM designed was evaluated based on performance indexes. From the analysis obtained, the PMLSM designed was compared with the previous designed PMLSM and the commercialized PMLSM.

4.1 Effect of Yoke Thickness, t_y to Thrust Characteristics

Figure 8 shows the magnetic flux density, B distribution of the PMLSM designed in first stage. Figure 8 shows that the increment of the stator yoke thickness, t_{y2} (region 1) decreased the value of magnetic flux density, B . Based on the magnetic flux density, B profile in Fig. 8, the corresponding thrust profile of the designed PMLSM is plotted in Fig. 9. Figure 9 shows that the thrust, F decreased as the magnetic flux density, B decreased. However, to choose the best model in first stage, the model with insignificant thrust, F decrement is chosen.

Based on the thrust taken at current, I equal to 3A as shown in Fig. 9(a), the highest thrust was produced by the model of $t_{y2} = 2$ mm with the value of maximum thrust 313 N. The thrust produced by the models were decreased as the thickness of the stator yoke, t_{y2} increased. The decrement of the thrust is represented by the average thrust as shown in the Fig. 9(b) where from the Fig. 9(b), the highest average thrust was produced by the original model, $t_{y2} = 2$ mm with $F_{\text{ave}} = 193$ N at current, I equal to 3A. The average thrust of the second model, $t_{y2} = 3$ mm decreased by 14% from the first model with average thrust, F_{ave} value of 166 N while the thrust of third model, $t_{y2} = 4$ mm and fourth model, $t_{y2} = 5$ mm decreased by 45% and 76% respectively from the first model.

4.2 Effect of Stator Slot Opening to Thrust and Cogging Characteristics

Figure 10 shows the thrust characteristics of several models designed taken at current, I equal to 3A. The thrust characteristics consist of thrust, F and cogging force, F_{cog} taken along the PMLSM displacement, x . From Fig. 10(a) it shows that as the length of stator slot opening, l_t increased, the thrust production decreased. From Fig. 10(a), the models that produced the highest thrust are model of $l_t = 2.5$ mm with the maximum thrust value more than 290 N. On the other hand, the models of $l_t = 9.5$ mm produced

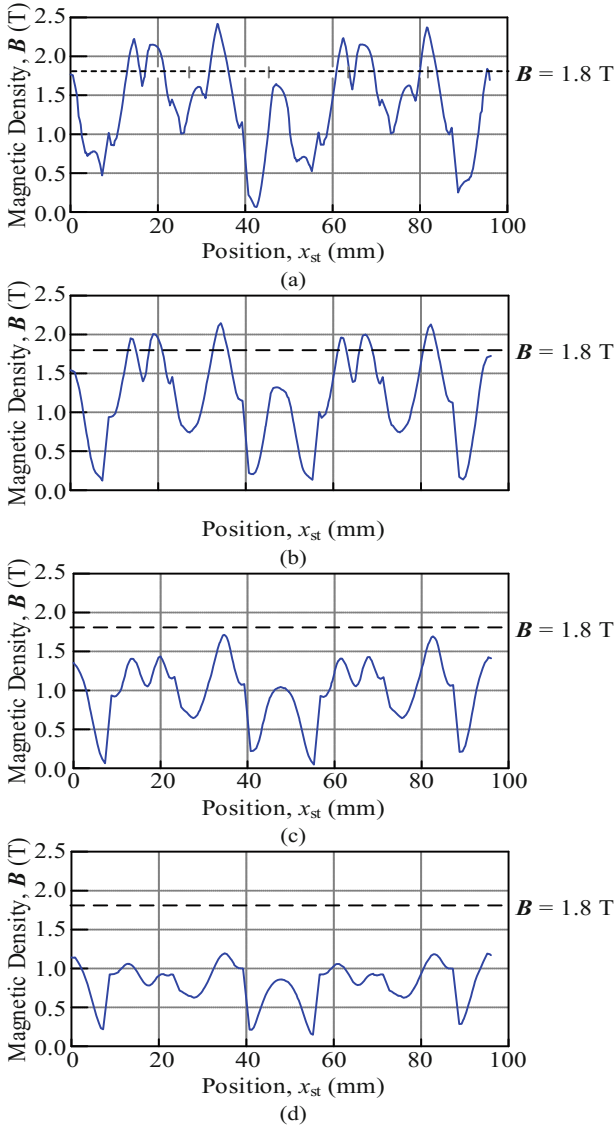


Fig. 8. Magnetic flux density, B distribution at region 1. (a) $t_{y2} = 2$ mm, (b) $t_{y2} = 3$ mm, (c) $t_{y2} = 4$ mm, (d) $t_{y2} = 5$ mm.

the lowest peak thrust with the value lower than 100 N. Figure 10(b) shows the cogging force, F_{cog} produced by the models designed. The model of $l_t = 7.5$ mm produced the highest cogging compared with other models with value more than 185 N at peak. Meanwhile, the models of $l_t = 1.5$ mm produced the lowest cogging with value of cogging lower than 100 N at peak. High cogging value influenced the thrust value where the higher the cogging the lower the thrust value and this is shown in Fig. 10.

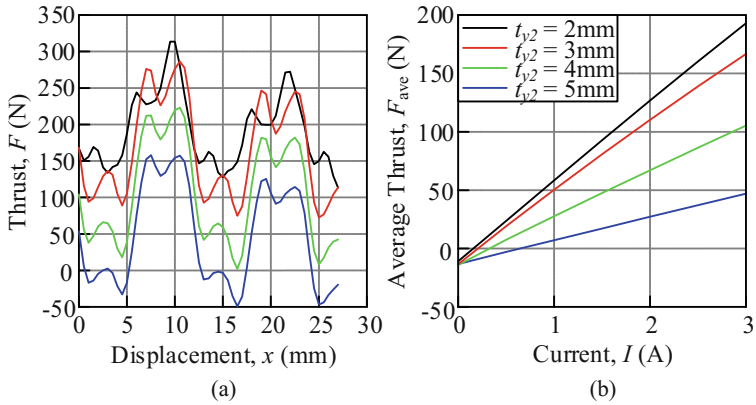


Fig. 9. PMLSM thrust characteristics in stage 1. (a) Thrust at 3A, (b) Average thrust.

Based on the thrust characteristics in Fig. 10, the thrust ratio has been calculated and presented in contour plot as shown in Fig. 11. There are two categories of thrust ratio which is thrust ratio of peak thrust, F_{max} to cogging force, F_{cog} and average thrust, F_{ave} to cogging force, F_{cog} . High thrust ratio designates high thrust, F production with low cogging force, F_{cog} . From Fig. 11 the high ratio value are represents by the red region while the low ratio value represents by dark blue region. The highest ratio of $F_{ave}:F_{cog}$ is 1.8439 whereas the highest ratio of $F_{max}:F_{cog}$ is 3.0469 produced by model $l_t = 1.5$ mm, $h_t = 1$ mm. The model $l_t = 9.5$, $h_t = 2$ mm has the lowest peak thrust to cogging which is $F_{max}:F_{cog}$ equal to 0.9352 while model $l_t = 9.5$ mm, $h_t = 3$ mm has the lowest average thrust to cogging ratio which is $F_{ave}:F_{cog}$ equal to -0.0374 . The negative value of ratio produced by the negative average thrust of models $l_t = 9.5$ mm.

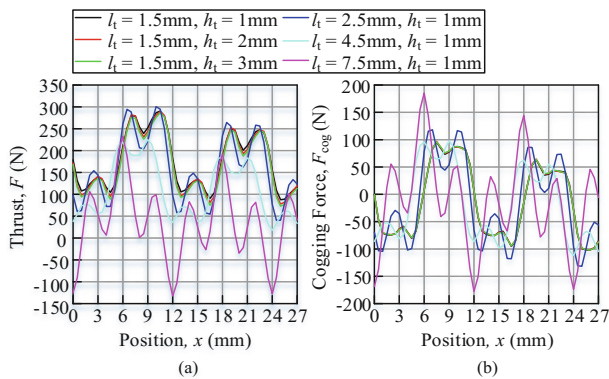


Fig. 10. PMLSM thrust characteristics. (a) Thrust characteristics at 3A, (b) Cogging force at 0A.

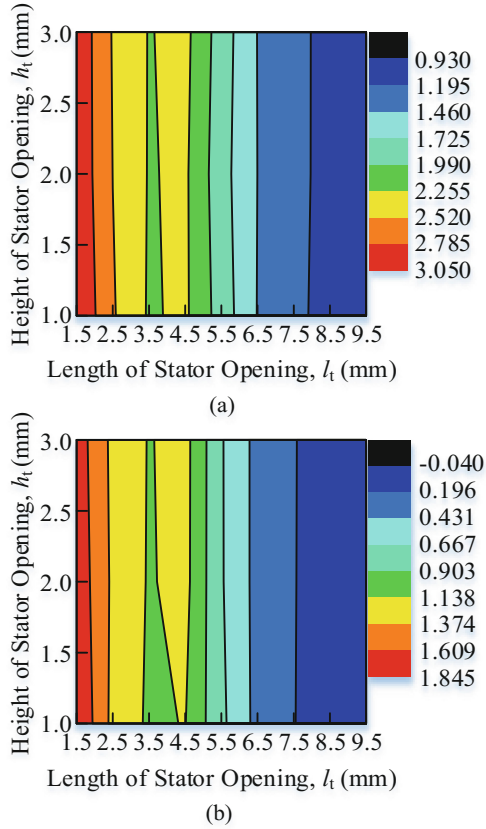


Fig. 11. PMLSM thrust ratio. (a) $F_{\max}: F_{\text{cog}}$, (b) $F_{\text{ave}}: F_{\text{cog}}$. (Color figure online)

4.3 Performance Index Comparison of PMLSM

Normally, the performance of the PMLSM is evaluated using thrust, F . However, thrust, F is affected by current, I , input power, P and motor volume, V_{mot} . Some researchers are suggesting several other performance characteristics such as spring constant, electrical time constant and mechanical time constant [6]. These parameters are related to dynamic performance. Therefore, in this paper, the performance indexes are implemented to make the comparison between PMLSMs valid. The performance indexes are thrust constant, k_f [7], motor constant, k_m and motor constant square density, G [8]. These performances indexes are calculated using Eqs. 1, 2 and 3.

$$k_f = \frac{F}{I} \quad (\text{N/A}) \tag{1}$$

$$k_m = \frac{F}{\sqrt{P}} \quad (\text{N}/\sqrt{\text{W}}) \tag{2}$$

$$G = \frac{F^2}{PV_{\text{mot}}} \quad (\text{N}^2/\text{Wm}^3) \quad (3)$$

where k_f is the thrust constant in (N/A), F is the average thrust in (N), I is the current in each coil in (A), k_m is the motor constant in (N/ $\sqrt{\text{W}}$), P_{in} is the input power in (W), G is the motor constant square density in (N²/Wm³) and V_{mot} is the motor volume in (m³).

Table 2. Performance indexes comparison of PMLSM.

Model	F_{ave} (N)	k_f ($\frac{\text{N}}{\text{A}}$)	k_m ($\frac{\text{N}}{\sqrt{\text{W}}}$)	$G \times 10^3$ ($\frac{\text{N}^2}{\text{Wm}^3}$)
Commercialized PMLSM	13	17	3	100
PMLSM as in [1]	193	64	8.52	385
Designed PMLSM	176	59	8.54	387

Table 2 shows the performance indexes comparison of three categories of the PMLSM. They are commercialized PMLSM that has similar volume with the designed PMLSM, the PMLSM as in [1] and the PMLSM designed in this paper.

The commercialized PMLSM with similar volume, V_{mot} has the lowest thrust, F which is 13 N hence produced the lowest thrust constant, k_f . Compared to the PMLSM as in [1], the designed PMLSM produced lower thrust, F hence produced lower thrust constant, k_f . The thrust constant produced by the PMLSM as in [1] and designed PMLSM is 64 N/A and 59 N/A respectively. However, the designed PMLSM produces higher motor constant, k_m and motor constant square density, G compared to the PMLSM as in [1]. Motor constant, k_m produced by PMLSM as in [1] is 8.52 N/ $\sqrt{\text{W}}$ while the designed PMLSM produced motor constant, k_m equal to 8.54 N/ $\sqrt{\text{W}}$. Motor constant, k_m represents the thrust sensitivity against input power. This means that the designed PMLSM can produced higher current at lower input power, P compared to the other PMLSM. The designed PMLSM produced the highest motor constant square density, G of $387 \times 10^3 \text{ N}^2/\text{Wm}^3$. On the other hand, the factor of linear motor volume, V_{mot} is considered through motor constant square density, G . The motor constant square density, G produced by the designed PMLSM represents that the model produced higher thrust at lower input power, P and smaller volume of the motor, V_{mot} compared with the other two models. However, in this case, since the volume, V_{mot} of the PMLSM as in [1] and the designed PMLSM is the same, the factors considered in the motor constant square density, G is input power, P .

5 Conclusion

The design of the PMLSM stator has been completed in two stages. In the first stage, the stator yoke thickness, t_{y2} has been designed to eliminate the magnetic flux density, B saturation of the PMLSM as in [1]. In the PMLSM as in [1], the magnetic flux density, B saturation occur at current, $I = 1.5\text{A}$. In the first stage, the magnetic flux

density, B decreased as the yoke thickness, t_{y2} was increased. The decrement of magnetic flux density, B resulted in reduction of the thrust, F produced. Therefore, in the first stage, the best model is chosen based on the model that produced insignificant thrust, F reduction. Model $t_{y2} = 3$ mm has been chosen as the best model in the first stage with the thrust, F production of 269 N at current, $I = 3$ A. In the second stage, the PMLSM design was focused on stator slot opening where the parameters involved are length of stator slot opening, l_t and height of stator slot opening, h_t . In the second stage, the aim of the design is to increase the ratio of thrust, F to cogging force, F_{cog} . This ratio performance is presented in the contour plot. Based on the thrust ratio, the model of $l_t = 1.5$ mm, $h_t = 1$ mm was chosen as the final model. The final model then was compared with the PMLSM as in [1] and the commercialized PMLSM in terms of performance index. Based on the comparison, the thrust, F produced by the final PMLSM is lower compared to the PMLSM as in [1]. As the thrust, F is low, the thrust constant, k_f also low correspondingly. However, the designed PMLSM produced higher motor constant, k_m and motor constant square density, G compared to the PMLSM as in [1].

Acknowledgments. The authors would like to thank Ministry of Education & Universiti Teknikal Malaysia Melaka (UTeM) for providing PJP/2016/FKE/HI5/S01478.

References

1. Azhar, F., Wakiwaka, H., Tashiro, K., Nirei, M.: Design and performance index comparison of the permanent magnet linear motor. *Prog. Electromagn. Res. M* **43**, 101–108 (2015)
2. Omura, M., Shimono, T., Fujimoto, Y.: Thrust characteristics improvement of a circular shaft motor for direct-drive applications. *IEEE Trans. Ind. Appl.* **51**(5), 3647–3655 (2015)
3. Vărățiceanu, B.D., Minciunescu, P.A.: Modeling and analysis of dual-sided coreless linear synchronous motor. *Rev. Roum. Sci. Tech.: Se.* **60**, 17–27 (2015)
4. Chen, Q., Liu, G., Zhao, W., Shao, M., Liu, Z.: Design and analysis of the new high-reliability motors with hybrid permanent magnet material. *IEEE Trans. Magn.* **50**(12), 1–10 (2014)
5. Patel, A.N.: Influence of stator teeth shaping on cogging torque of radial flux permanent magnet brushless DC motor. In: 2016 Biennial International Conference on Power and Energy Systems: Towards Sustainable Energy (PESTSE), pp. 1–4 (2016)
6. Norhisam, M., Firdaus, R.N., Azhar, F., Mariun, N., Aris, I., Abdul, R.J.: The analysis on effect of thrust constant, spring constant, electrical time constant, mechanical time constant to oscillation displacement of slot-less linear oscillatory actuator. In: IEEE 2nd International Power and Energy Conference (PECON), pp. 1076–1081 (2008)
7. Wakiwaka, H., Ninomiya, T., Oda, J., Morimura, T., Yamada, H.: Evaluation of the thrust constant of a linear DC motor for a pen recorder. *IEEE Transl. J. Magn. Japan* **9**(6), 104–109 (1994)
8. Mizuno, T., Kawai, M., Tsuchiya, F., Kosugi, M., Yamada, H.: An examination for increasing the motor constant of a cylindrical moving magnet-type linear actuator. *IEEE Trans. Magn.* **41**(10), 3976–3978 (2005)